

# Resource limitation of autotrophs and heterotrophs in boreal forest headwater streams

Sophie A. Weaver<sup>1,2,3</sup> and Jeremy B. Jones Jr<sup>1,4</sup>

<sup>1</sup>Institute of Arctic Biology and Department of Biology and Wildlife, University of Alaska Fairbanks, 311 Irving 1 Building, 2140 Koyukuk Drive, Fairbanks, Alaska 99775 USA

<sup>2</sup>Alaska Department of Fish and Game, Commercial Fisheries Division, 351 Research Court, Kodiak, Alaska 99615 USA

**Abstract:** Autotrophic and heterotrophic microbes in stream biofilms dominate biogeochemical cycling and rely on nutrient and energy resources for growth and productivity. In the boreal forest, variation in these resources can originate from permafrost distribution and controls competition for nutrients between stream autotrophs and heterotrophs. We investigated which resources control nutrient uptake and metabolism in headwater stream biofilms of subarctic Alaska, USA, and how resource availability affects competition for inorganic nutrients. We hypothesized that the competitive outcome between autotrophs and heterotrophs for inorganic nutrients would be dependent on availability of organic C, or inorganic nutrients (N and P). To test our hypotheses, we measured resource limitation at the patch and reach scales along a permafrost gradient in interior Alaska. At the patch scale, nutrient diffusing substrata revealed that, secondary to light, N and P were colimiting to autotrophic growth, whereas C was primarily limiting to heterotrophic respiration. In the presence of labile C, heterotrophs exhibited a larger response to nutrient enrichment and outcompeted autotrophs for inorganic nutrients. At the reach scale, light availability had the largest influence on nutrient uptake, but inorganic nutrients were also important. The positive response to increased nutrient and C availability at the patch scale suggests that the predicted increase in exports into fluvial networks with permafrost degradation will alter biofilm structure and function. Ultimately, biofilm communities will shift to more heterotroph-dominated patches if heterotrophs outcompete autotrophs for inorganic nutrients. As permafrost thaws and nutrients and organic C mobilize into streams, nutrient uptake dynamics and competition within biofilms will be altered, affecting nutrient use and export.

**Key words:** phosphorus, dissolved organic carbon, biofilm, autotroph, heterotroph, boreal, nutrient diffusing substrata

Stream biofilms dominate biogeochemical processes in stream channels (Battin et al. 2016) through nutrient transformations (Van Horn et al. 2011), extracellular enzyme production (Romani and Sabater 2001), and organic matter decomposition (Battin et al. 2008). Within biofilms, photoautotrophs (e.g., algae and cyanobacteria) require light to fix C through photosynthesis (Hill et al. 2009), whereas heterotrophic organisms (e.g., fungi, bacteria, and Archaea) use allochthonous- or autochthonous-derived dissolved organic C (DOC) as an energy source for heterotrophic respiration (HR; Bernhardt and Likens 2002, Robbins et al. 2017). Both autotrophs and heterotrophs use inorganic nutrients for ecosystem respiration (ER) and biosynthesis, and heterotrophs can additionally utilize organic nutrients (Battin et al. 2016). The availability of nutrient resources and or-

ganic C resources, along with abiotic controls such as light, controls the competitive outcome between autotrophs and heterotrophs in biofilms.

Because microbes must assimilate nutrients at relatively fixed ratios, nutrient stoichiometry of organic C, N, and P in the water column affects nutrient uptake rates (Schade et al. 2011, Piper et al. 2017), and nutrients can be colimiting (Elser et al. 2007). Heterotrophs must maintain a fairly consistent nutrient stoichiometry, and organic C uptake is often limited by ambient nutrient concentrations (Ziegler et al. 2009). A more plastic nutrient stoichiometry allows autotrophs to utilize limited inorganic nutrients (Sterner et al. 1998) if light is sufficient. In shaded channels with low primary production, heterotrophic bacteria and fungi predominantly use allochthonous organic matter for HR

E-mail addresses: <sup>3</sup>saweaiver2@alaska.edu; <sup>4</sup>jbjonesjr@alaska.edu

Received 1 October 2021; Accepted 12 May 2022; Published online 14 September 2022. Associate Editor, Nicholas G. Aumen.

*Freshwater Science*, volume 41, number 4, December 2022. © 2022 The Society for Freshwater Science. All rights reserved. Published by The University of Chicago Press for the Society for Freshwater Science. <https://doi.org/10.1086/722256> 000

(Kaplan et al. 2008), whereas in open-channel streams with higher light, autotrophic algae and cyanobacteria dominate organic C fixation and exudation of autochthonous C to heterotrophs for HR (Thorp and Delong 2002, Dodds 2007). Temperature has both direct and indirect effects on metabolic rates, which, in turn, control nutrient use and assimilation (Demars et al. 2011, Cross et al. 2015). Therefore, in boreal headwater streams, autotrophs and heterotrophs compete for inorganic nutrients with the outcome of competition dependent on light availability, labile dissolved organic matter (DOM) quality and abundance, inorganic nutrient concentrations, and temperature (Fig. 1).

In high-latitude streams draining catchments underlain by discontinuous permafrost, the extent of the perennially frozen ground affects the available resources for microbes. In interior Alaska, USA, and western Siberia, Russia, streams draining low permafrost or permafrost-free catchments have higher  $\text{PO}_4^{3-}$  and  $\text{NO}_3^-$  concentrations than streams draining catchments dominated by permafrost (Jones et al. 2005, Frey et al. 2007a, b). These increased nutrient concentrations can arise from deepening permafrost active-layer depth due to warming, which can alter vegetation and soil conditions, increasing microbial decomposition and turnover of nutrient pools within the organic soil layer, with likely export into streams (Davidson and Janssens 2006). Higher erosion caused by reduced streambank stability from per-

mafrost loss can also increase nutrient exports into streams through the release of higher concentrations of organic matter, inorganic nutrients, and major ions into catchments (Kokelj and Jorgenson 2013).

Concentration and bioavailability of C reveals an opposite pattern than nutrients in permafrost-impacted watersheds. Streams draining catchments with low permafrost extent contain a lower concentration of DOC than streams draining catchments underlain with higher permafrost extent, but a higher proportion of this DOC is labile (Balcarczyk et al. 2009). This highly degradable labile DOC (LDOC) could be attributed to increased active microbial decomposition in unfrozen soils. As the climate warms and permafrost thaws, variation in resource availability (e.g., light, organic C) will likely be reflected as temporal changes in nutrient fluxes and concentrations (Frey and McClelland 2009). For example, in the Kuparuk River in Arctic Alaska, a small increase in dissolved P concentration ( $10 \mu\text{g PO}_4^{3-}\text{-P/L}$ ) increased algal biomass by an order of magnitude (Peterson et al. 1985, 2002, Slavik et al. 2004). In response to this increase in algal biomass, gross primary production (GPP) also increased, resulting in elevated HR and microbial biomass. This finding suggests that heterotrophic microorganisms shifted from assimilating predominately allochthonous C to newly fixed autochthonous C (Peterson et al. 1985).

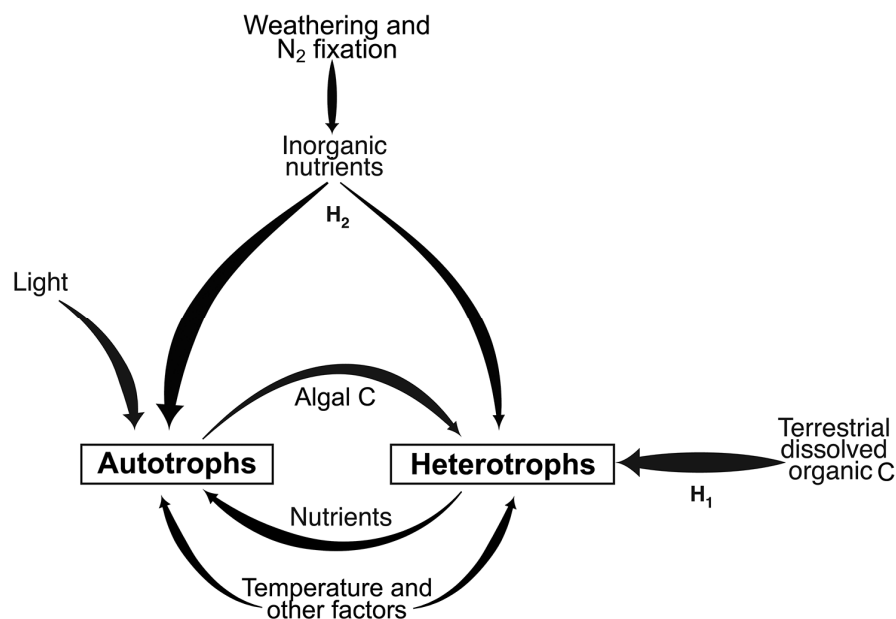


Figure 1. Conceptual diagram with experimental hypotheses outlines controls on autotrophs and heterotrophs in boreal forest streams (modified from Currie 1990). Experimental hypotheses predict that autotrophic and heterotrophic microorganisms compete for inorganic nutrients with competition outcome (e.g., productivity rates and biomass) dependent on the quality and quantity of dissolved organic matter ( $H_1$ ) or inorganic nutrient concentration ( $H_2$ ). Arrow size reflects predicted strength of hypothesized relationships. Other factors affecting autotrophic and heterotrophic growth and productivity may include disturbance by grazers, stream discharge, etc.

Using both patch- and reach-scale approaches, we examined how variation in water chemistry affects competition between autotrophs and heterotrophs in streams draining catchments with varying permafrost extent and light availability. The objectives of this study were to determine 1) which nutrient and energy resources control autotrophic and heterotrophic activity and biomass in boreal forest headwater streams and 2) how these resources affect competition for inorganic nutrients between autotrophs and heterotrophs. We hypothesized that autotrophs and heterotrophs compete for inorganic nutrients with the outcome dependent on DOM quality and quantity or inorganic nutrient concentration (Fig. 1). We predicted that P was the limiting nutrient for microbial growth and productivity in these headwater streams. We further predicted that in conditions favoring heterotrophs, bioavailable organic C would allow heterotrophs to outcompete autotrophs, regardless of inorganic nutrient concentration. In conditions favoring autotrophs, however, we predicted that inorganic nutrient availability would control this competition but that heterotrophs might, in turn, utilize autotrophs as a bioavailable C source.

## METHODS

### Study design

To test our hypotheses, we quantified LDOC through 40-d lab incubations to measure C loss over time, analyzed streamwater chemistry to determine how autotrophs and heterotrophs respond to varying ambient nutrient concentration, and conducted 2 separate experiments in streams with differing water chemistry and light conditions. To examine resource limitation at the patch scale, we deployed nutrient diffusing substrata (NDS) in 4 study streams in the Caribou-Poker Creeks Research Watershed (CPCRW) in central Alaska, USA, in shaded and high-light stream reaches for 20 d in July 2018 (4 streams, 6 nutrient treatments, 2 light treatments, 10 replicates/treatment: 120 NDS/stream, total = 480 NDS) followed by lab metabolism incubations (GPP, respiration: ER and HR,  $n = 5$ ). Tarps were used to completely block light penetration to shaded NDS and the surrounding stream channel. We also measured chlorophyll *a* (Chl *a*;  $n = 9$ ) to quantify nutrient limitation and examine the competitive interactions between autotrophs and heterotrophs at the patch scale. For these analyses we used mixed-effects models followed by analysis of variance (ANOVA) and pairwise comparisons. At the reach-scale, we conducted nutrient uptake experiments in August and September of 2017 and 2018. We quantified nutrient and labile C uptake in dark (2018) and light (2017 and 2018) conditions to try to separate autotrophic and heterotrophic processes. Dark and light experiments were conducted with various nutrient amendments, with 8 and 9 total experimental combinations (i.e., reach  $\times$  nutrient;  $n = 1$ ) in 2017 and 2018, respectively. We did not statisti-

cally analyze these data because we did not replicate the experiment.

### Study site

We conducted our research at the CPCRW (lat 65.15°N, long 147.50°W) located 50 km northeast of Fairbanks, Alaska, USA (Fig. 2). The CPCRW is a 104-km<sup>2</sup> research watershed underlain with discontinuous permafrost with no direct human influences other than scientific research. The climate is continental with cold winters (January mean:  $-21^{\circ}\text{C}$ ), warm summers (July mean:  $16^{\circ}\text{C}$ ), and low annual precipitation (yearly mean: 411 mm). Stream temperature typically ranges from 2 to  $5^{\circ}\text{C}$ . Well-drained inceptisols with thin organic horizons and loamy texture are typical of south-facing slopes, whereas poorly drained gelisols with thick organic horizons underlain with permafrost dominate north-facing slopes because of solar aspect. Permafrost across northern slopes and valley bottoms is unstable, and an estimated 2% of CPCRW permafrost has thawed over the past century (Hinzman et al. 2005).

Headwater streams sampled in this study were all 1<sup>st</sup>-order streams (C1, C2, C3, and C4; Fig. 2) located in catchments underlain by variable permafrost extent (4–53% cover; Table 1) with varying water chemistry (Table 2). Streams draining catchments underlain with high permafrost extent are characterized by lower  $\text{NO}_3^-$  and higher DOC concentrations than streams draining catchments underlain with lower permafrost extent (Petrone et al. 2006, Balcarczyk et al. 2009).

### Water physicochemical analysis

We collected ambient water chemistry data at each CPCRW stream throughout the 2017 and 2018 field seasons. Autosamplers (ISCO 3700; Teledyne Technologies, Thousand Oaks, California) collected daily water samples, and we manually collected additional biweekly grab samples in high-density polyethylene (HDPE) bottles. Upon field collection, we placed water samples in a cooler, transported them to the lab, filtered the samples to 1.0  $\mu\text{m}$  within 24 h, and refrigerated them at  $4^{\circ}\text{C}$ . We froze water samples ( $-18^{\circ}\text{C}$ ) for future analysis that could not be analyzed within 5 d of collection.

We analyzed each water sample for total dissolved P, soluble reactive P (SRP), total dissolved N, DOC, anions ( $\text{Cl}^-$ ,  $\text{NO}_3^-$ ,  $\text{NO}_2^-$ ), cations ( $\text{NH}_4^+$ ), specific ultraviolet absorbance at 254 nm (SUVA<sub>254</sub>), and pH. We used the colorimetric molybdate blue method with a spectrophotometer (5-cm cell path, limit of quantification [LOQ] 0.7  $\mu\text{g P/L}$ ; UVmini-1240; Shimadzu, Kyoto, Japan) to quantify SRP, and we measured total dissolved P as SRP following persulfate digestion (Murphy and Riley 1962). We calculated total organic P as the difference between total dissolved P and SRP. We used a Shimadzu total organic C (TOC) analyzer (TOC-5000) to measure DOC (Merriam et al. 1996),

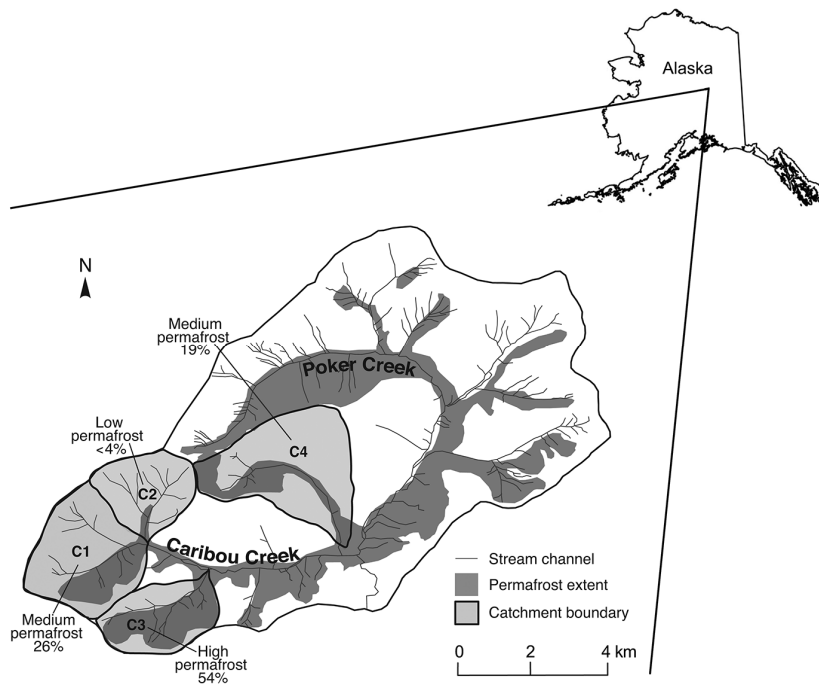


Figure 2. Map of the Caribou-Poker Creeks Research Watershed in central Alaska, USA. Black branching lines indicate stream channels, dark gray regions represent land area underlain by permafrost, and light gray regions represent study-stream catchment boundaries. Stream names are indicated as C1 through C4.

and we used a chemiluminescent N detector (model 7050; Antek Instruments, Houston, Texas) to measure total dissolved N following combustion to  $\text{NO}_x$ . We used ion chromatography (Dionex DX-320; Thermo Fisher Scientific, Waltham, Massachusetts) to quantify anions and cations. We calculated dissolved organic N as the difference between total dissolved N and dissolved inorganic N ( $\text{NO}_3^- + \text{NO}_2^- + \text{NH}_4^+$ ). We quantified SUVA by measuring absorbance at 254 nm (1-cm cell path; UVmini-1240). We then calculated  $\text{SUVA}_{254}$ , a measure of DOM aromaticity (Weishaar et al. 2003), by dividing UV absorbance at 254 nm by DOC concentration (mg C/L).

For nutrient uptake experiments, we quantified  $\text{NH}_4^+$ ,  $\text{Cl}^-$ , SRP, and DOC. For  $\text{NH}_4^+$  we used the phenol hypochlorite method (Solorzano 1968) with automated colorimetry (LOQ 0.01 mg N/L; SmartChem® 170; Westco Scientific Instruments, Brookfield, Connecticut). For  $\text{Cl}^-$  we used the mercuric thiocyanate method (Zall et al. 1956). For samples with high SRP concentration (6.0–100  $\mu\text{g P/L}$ ), we used the colorimetric molybdate blue method with a plate reader (LOQ 5.15  $\mu\text{g P/L}$ ; Synergy™ HT; BioTek Instruments, Winooski, Vermont) to measure SRP, whereas for samples with lower SRP concentration (start and end of break-through curve; <6.0  $\mu\text{g P/L}$ ), we measured SRP

Table 1. Catchment characteristics at the Caribou-Poker Creeks Research Watershed located northeast of Fairbanks, Alaska, USA. Includes mean ( $\pm\text{SE}$ ) dissolved organic C (DOC) lability ( $n = 8$ ), mean ( $\pm\text{SE}$ ) DOC concentration ( $n = >16$ ), and specific UV absorbance at 254 nm ( $\text{SUVA}_{254}$ ;  $n = 40$ ) in study streams during nutrient diffusing substrata incubations in July 2018. C loss measured as decrease in DOC over 40-d lab incubations.

Stream	Catchment characteristics				C lability			
	Area (km <sup>2</sup> )	Elevation (m)	Aspect	Permafrost (% cover)	DOC (mg/L)	C loss (mg C L <sup>-1</sup> d <sup>-1</sup> )	C loss %	SUVA <sub>254</sub> (L mg C <sup>-1</sup> m <sup>-1</sup> )
C1	6.7	325	E	26	2.5 $\pm$ 0.06	0.0061 $\pm$ 0.001	10.92	3.45 $\pm$ 0.06
C2	5.2	323	S	4	2.0 $\pm$ 0.13	0.0045 $\pm$ 0.001	10.21	3.00 $\pm$ 0.13
C3	5.7	274	NE	53	3.2 $\pm$ 0.12	0.0038 $\pm$ 0.001	5.28	3.24 $\pm$ 0.07
C4	10.0	226	SSE	19	1.6 $\pm$ 0.05	0.0015 $\pm$ 0.001	4.21	2.57 $\pm$ 0.08

Table 2. Mean ( $\pm$  SE) ambient water chemistry data from summer 2017 and 2018, and 20-d nutrient diffusing substrata (NDS) incubations at the Caribou-Poker Creeks Research Watershed in central Alaska, USA. Water chemistry was quantified from autosampler and mainstem water samples ( $n > 16$ ). Discharge and temperature in streams C2, C3, and C4 were measured continuously throughout the field season ( $n > 6000$ ). Dissolved organic N (DON) and total organic P (TOP) were calculated, whereas soluble reactive P (SRP) and dissolved organic C (DOC) were quantified directly. The 2017 season is included to show annual variation in water chemistry. For SRP, TOP, pH, and DOC, sample sizes were 16 to 20/field season (depending on frequency of field sampling) and DON,  $\text{NO}_3^-$ , and  $\text{NH}_4^+$  were sampled using autosamplers for sample sizes of  $\sim 100$ /season. – indicates no data.

Year	Stream	Discharge (L/s)	Temperature (°C)	pH	$\text{NO}_3^-$ ( $\mu\text{g N/L}$ )	$\text{NH}_4^+$ ( $\mu\text{g N/L}$ )	DON ( $\mu\text{g N/L}$ )	SRP ( $\mu\text{g P/L}$ )	TOP ( $\mu\text{g P/L}$ )	DOC ( $\text{mg C/L}$ )
2017	C1	49.2 <sup>a</sup>	2.2 <sup>a</sup> $\pm$ 0.26	6.9 $\pm$ 0.04	331.7 $\pm$ 5.18	37.8 $\pm$ 3.40	39.9 $\pm$ 7.37	2.0 $\pm$ 0.20	2.4 $\pm$ 0.58	3.2 $\pm$ 0.23
	C2	28.2 $\pm$ 0.01	3.5 $\pm$ 0.01	7.2 $\pm$ 0.04	502.3 $\pm$ 10.03	42.0 $\pm$ 4.27	49.9 $\pm$ 12.71	1.6 $\pm$ 0.18	2.1 $\pm$ 0.38	2.5 $\pm$ 0.14
	C3	34.1 $\pm$ 0.01	2.8 $\pm$ 0.01	7.1 $\pm$ 0.03	502.7 $\pm$ 9.28	53.8 $\pm$ 4.40	37.1 $\pm$ 7.43	1.9 $\pm$ 0.18	2.7 $\pm$ 0.45	4.1 $\pm$ 0.22
	C4	57.3 $\pm$ 0.01	3.5 $\pm$ 0.01	7.5 $\pm$ 0.04	627.3 $\pm$ 6.23	43.2 $\pm$ 3.64	38.2 $\pm$ 10.56	2.6 $\pm$ 0.25	2.5 $\pm$ 0.11	2.0 $\pm$ 0.21
2018	C1	173.0 <sup>a</sup>	3.6 <sup>a</sup> $\pm$ 0.26	6.8 $\pm$ 0.04	301.5 $\pm$ 9.14	28.3 $\pm$ 4.14	75.8 $\pm$ 4.56	2.5 $\pm$ 0.30	2.5 $\pm$ 0.59	2.7 $\pm$ 0.08
All summer	C2	64.0 $\pm$ 0.01	5.0 $\pm$ 0.01	7.1 $\pm$ 0.05	633.8 $\pm$ 12.87	26.5 $\pm$ 2.62	89.2 $\pm$ 7.19	3.6 $\pm$ 0.71	2.9 $\pm$ 0.77	2.1 $\pm$ 0.07
	C3	75.1 $\pm$ 0.01	1.8 $\pm$ 0.01	7.1 $\pm$ 0.03	555.7 $\pm$ 5.74	35.5 $\pm$ 4.03	98.8 $\pm$ 7.34	3.3 $\pm$ 0.50	2.2 $\pm$ 0.67	3.6 $\pm$ 0.11
	C4	115.3 $\pm$ 0.01	3.3 $\pm$ 0.01	7.3 $\pm$ 0.03	657.6 $\pm$ 4.50	29.4 $\pm$ 3.50	79.4 $\pm$ 6.23	3.0 $\pm$ 0.32	2.0 $\pm$ 0.56	1.8 $\pm$ 0.05
	C1	– <sup>a</sup>	4.2 <sup>a</sup> $\pm$ 0.14	6.8 $\pm$ 0.04	260.4 $\pm$ 2.52	22.1 $\pm$ 5.61	74.2 $\pm$ 14.4	2.7 $\pm$ 0.43	0.6 $\pm$ 0.34	2.5 $\pm$ 0.06
20-d NDS	C2	63.0 $\pm$ 0.02	5.1 $\pm$ 0.02	7.1 $\pm$ 0.05	609.9 $\pm$ 9.71	19.0 $\pm$ 3.45	72.1 $\pm$ 11.67	5.5 $\pm$ 1.82	0.7 $\pm$ 0.17	2.0 $\pm$ 0.13
	C3	71.4 $\pm$ 0.02	2.0 $\pm$ 0.02	7.1 $\pm$ 0.02	550.9 $\pm$ 2.12	38.9 $\pm$ 0.58	117.7 $\pm$ 10.16	2.8 $\pm$ 0.28	1.3 $\pm$ 0.19	3.2 $\pm$ 0.12
	C4	106.3 $\pm$ 0.02	3.5 $\pm$ 0.02	7.4 $\pm$ 0.02	658.6 $\pm$ 3.01	26.0 $\pm$ 4.08	58.6 $\pm$ 6.29	3.6 $\pm$ 0.75	1.1 $\pm$ 0.16	1.6 $\pm$ 0.05

<sup>a</sup> C1 is the only stream where discharge and temperature were not measured continuously using pressure transducers and conductivity loggers throughout the summer field season. Here, stream discharge was manually measured ( $n = 1$ ) using slugs during August uptake experiments and temperature was recorded during site visits ( $n = 18$ ). C1 discharge was not measured during the 20-d NDS deployment.

using the same method on a UVmini-1240 spectrophotometer. DOC was measured using the same methods as the ambient water chemistry samples above.

We monitored physical stream characteristics throughout the summer field seasons. We calculated stream discharge by continuously measuring stream stage height with Levelogger<sup>®</sup> 5 pressure transducers (model 3001; Solinst<sup>®</sup>, Georgetown, Ontario, Canada). Continuous discharge was modeled from stage height and the rating curves for each of the streams. Likewise, in all streams other than C1, we continuously monitored conductivity and temperature throughout the field season with a HOBO<sup>®</sup> U24 conductivity logger (Onset<sup>®</sup> Computer Corporation, Bourne, Massachusetts). Temperature and conductivity were measured biweekly at C1.

### LDOC incubations

We quantified DOC loss due to microbial decomposition to determine how DOC lability varied among study streams. We measured LDOC in each study stream at the start and end of NDS deployment. We collected 4 replicate water samples from each stream's thalweg in acid-washed HDPE bottles. All water samples were filtered through 1.0- $\mu\text{m}$  glass-fiber filters (Type A/E; Pall<sup>®</sup> Corporation, Port Washington, New York) upon return to the lab. Within 24 h, we filtered samples to 0.22  $\mu\text{m}$  with polyethersulfone mem-

brane filters (MilliporeSigma<sup>®</sup>, Burlington, Massachusetts) to remove the microbial community. We placed these used 0.22- $\mu\text{m}$  filters in a beaker of Barnstead<sup>™</sup> Nanopure<sup>™</sup> water (Thermo Fisher Scientific;  $\sim 10$  mL Nanopure for each filter), swirled the beakers, and allowed the filters to soak to create a common microbial inoculum of all study streams. We then transferred filtered water samples in 100-mL volumes to 250-mL ashed glass incubation vials. We amended all incubation vials with nutrients to alleviate nutrient limitation of microbial decomposition in stream water by increasing ambient concentrations by 10  $\mu\text{mol}$   $\text{PO}_4^{3-}$  and 80  $\mu\text{mol}$  total of  $\text{NH}_4^+$  and  $\text{NO}_3^-$  (McDowell et al. 2006, Abbott et al. 2014). To ensure that all water samples were exposed to the same microbial community, we added 1 mL of the microbial inoculum to each incubation vial. We then capped the vials to eliminate water loss through evaporation and stored them in the dark at room temperature ( $\sim 19^\circ\text{C}$ ). We removed the caps weekly and wafted the vials to ensure that microbial processes were not constrained by low oxygen and to replenish oxygen into the head space.

To quantify C loss over time, we sampled 20 mL from each incubation vial at d 0, d 8, and d 40. We then filtered the samples to 0.22  $\mu\text{m}$  to remove inoculated bacterial communities and acidified the samples with 2N HCl to remove inorganic C and to preserve samples until TOC quantification. We placed samples in ashed glass scintillation vials,

stored them at room temperature in the dark ( $\sim 19^\circ\text{C}$ ), and quantified C loss within 3 mo. We calculated C loss as the change between initial and final TOC over time, averaged over the 4 incubation replicates. Any TOC remaining at d 40 was considered recalcitrant.

### Patch-scale experiment

**NDS** We constructed NDS with 2% agar solution and amended them with  $\text{NH}_4^+$  (N treatment: 0.5 mol  $\text{NH}_4\text{Cl}$ ), phosphate (P treatment: 0.5 mol  $\text{KH}_2\text{PO}_4$ ), acetate (C treatment: 0.5 mol  $\text{C}_2\text{H}_3\text{NaO}_2$ ), or combinations of these solutes (NP, NPC: each at 0.5 mol). Control (U) treatments contained unamended agar. We chose nutrient concentrations of 0.5 mol to remain consistent with previous studies (Tank and Dodds 2003, Reisinger et al. 2016, Burrows et al. 2017, Myrstener et al. 2018). Nutrient-amended agar for NPC treatments was altered to contain 3% agar to accommodate higher concentrations of nutrient salts (Tank et al. 2011). We prepared all agar treatments in the laboratory, poured the agar into 30-mL plastic cups with  $\sim 2.5\text{-cm}$  holes drilled into the center of the caps, and then allowed the agar to cool and solidify. Once solidified, we placed a fritted glass filter disk directly on the agar surface and capped the cups to secure the disks.

We deployed NDS on 6 July 2018, left them to incubate for 20 d, and checked them regularly throughout the incubation period to ensure NDS remained anchored to the streambed. We deployed the replicates of each NDS treatment (6 nutrient treatments, 2 light treatments, 10 replicates/treatment; 120 NDS/stream) by securely attaching each cup to L bars (grouped by light treatment, 60 shaded, 60 high light) with zip ties to prevent sample loss during instream incubations. We pounded rebar into the stream substrate and securely attached L bars to the rebar with zip ties. We positioned control treatments upstream of nutrient-enriched NDS to avoid any passive diffusion of nutrients downstream. We positioned NDS in clusters in the stream thalweg  $\sim 15$  to 30 cm under the stream surface to ensure light attenuation yet prevent desiccation during low flow. In high-light stream reaches, we pruned riparian vegetation around NDS-incubation sites to permit maximum sunlight to reach NDS within the channel. We covered shaded treatments with tarps immediately upon deployment. We used a light meter (LI-189 Quantum Radiometer Photometer; LI-COR® Biosciences, Lincoln, Nebraska,) to confirm that tarps blocked photosynthetically active radiation (PAR) in shaded treatments ( $\text{PAR} < 0.6 \mu\text{mol m}^{-2} \text{s}^{-1}$ ).

At the end of incubations, we removed the fritted glass filter disks with colonized biofilms from the agar surface of NDS cups and individually placed these disks into 50-mL centrifuge tubes. We then gently filled the centrifuge tubes by submersion in a bucket of fresh stream water and placed them in coolers for immediate transport to the lab. Not all NDS could be recovered at the end of the deploy-

ment, particularly in C2 and C4, with 10 sample sizes of 9 and 7 sample sizes of 8. In C4, we only recovered 4 replicated from the C high-light treatment.

**Patch-scale metabolism incubations** Upon return to the lab, centrifuge tubes containing colonized biofilms and stream water were refrigerated ( $\sim 4^\circ\text{C}$ ) overnight. The following day, we collected and transported fresh stream water from Caribou Creek to the lab for use during metabolism incubations (Fig. 2). We conducted metabolism experiments with 5 replicates/treatment following protocols from Johnson et al. (2009b) and Reisinger et al. (2016). To ensure high initial dissolved oxygen concentration, we saturated stream water with oxygen by bubbling air into experimental stream water prior to incubations. We then emptied the old water and refilled the centrifuge tubes, which contained the colonized biofilms, with fresh dissolved oxygen-saturated stream water, capped the tubes underwater to prevent air bubbles, and placed them in coolers ( $\text{PAR} < 0.5 \mu\text{mol m}^{-2} \text{s}^{-1}$ ). We measured dissolved oxygen at the start and end of 3-h incubations with a handheld ProODO optical dissolved oxygen meter (Yellow Springs Instruments, Yellow Springs, Ohio).

Within 12 h of dark incubations, we refilled centrifuge tubes containing individual fritted glass filter disks with fresh unfiltered stream water and followed the same protocol under high-light conditions. We placed the samples under full spectrum grow lights to simulate natural ambient light conditions observed in the field ( $\text{PAR} = \sim 200\text{--}300 \mu\text{mol m}^{-2} \text{s}^{-1}$ ) for additional 3-h incubations. All incubations were performed in the laboratory at room temperature ( $\sim 19^\circ\text{C}$ ).

We calculated respiration ( $R$ ;  $\mu\text{g O}_2 \text{ cm}^{-2} \text{ h}^{-1}$ ) as the loss of dissolved oxygen during dark incubations and net ecosystem production ( $NEP$ ;  $\mu\text{g O}_2 \text{ cm}^{-2} \text{ h}^{-1}$ ) as the change in dissolved oxygen during light incubations. We then calculated GPP ( $\mu\text{g O}_2 \text{ cm}^{-2} \text{ h}^{-1}$ ) as:

$$GPP = NEP + R. \quad (\text{Eq. 1})$$

Centrifuge tubes containing stream water alone were included in lab incubations to quantify  $R$  and  $NEP$  occurring in the water column ( $n = 5$ ); these values were subtracted from incubations of colonized biofilms. For metabolism incubations, NDS treatments deployed in high-light stream reaches include both autotrophic and heterotrophic respiration (ER), whereas NDS treatments deployed in shaded stream reaches reflect HR. Throughout this text, the term respiration refers to both ER and HR together. Immediately following metabolism incubations, we individually wrapped biofilm samples in aluminum foil, froze them ( $-80^\circ\text{C}$ ), and measured their  $\text{Chl } \alpha$  concentration within 3 mo, with 9 replicates treatment $^{-1}$  stream $^{-1}$ . We used a UVmini-1240 spectrophotometer to colorimetrically quantify  $\text{Chl } \alpha$  after

24-h acetone extractions on ice ( $\sim 2^\circ\text{C}$ ; Steinman et al. 2011).

**Patch-scale statistical analyses** We examined the effects of nutrient treatment (N, P, C, NP, NPC, or U) and shading effect (high light vs shaded) on response variables (GPP, Chl  $a$ , and respiration) and their interaction with linear mixed-effects models (LMM) which included stream as a random effect in the *lme4* package (version 1.1-28; Bates et al. 2015) in the statistical computing software R (version 4.0.4; R Project for Statistical Computing, Vienna, Austria). In separate LMMs for each response variable, we nested NDS replicates (i.e., did not treat them as true replicates) within nutrient treatment within high-light/shaded reaches (both fixed factors) within streams (random factor). Because of non-normality of residuals, we log transformed response variables prior to running LMMs. Next, we tested for differences among treatment means with Type III ANOVA using the Satterthwaite method for calculating approximate denominator degrees of freedom in the *lmerTest* package (version #1.1-29; Kuznetsova et al. 2020). We then used Tukey's honestly significant difference post-hoc comparisons to determine differences between treatments and shading effects across streams and considered effects to be different when they obtained  $p$ -values  $< 0.05$ .

To determine limitation of response variables, we followed Tank and Dodds (2003) to interpret the results of the ANOVAs (Table 3). To determine nutrient limitation by a single nutrient (N, P, or C), we compared treatments with unamended controls and determined primary limitation if only 1 nutrient (e.g., P) caused a positive response. We considered streams to be colimited when 1) multiple single nutrients (e.g., P and N) caused a positive response but those responses did not differ from each other or 2) no

single nutrient elicited a positive response but combinations of nutrient treatments (NP or NPC) were detectably greater than unamended controls. To determine secondary limitation, we compared nutrient amendments with multiple nutrients (NP and NPC) with the primary limiting nutrient. We considered light to be the primary control of autotrophic productivity or biomass when none of the shaded treatments showed a positive response to nutrient amendment when compared with shaded unamended controls.

We calculated response ratios (RR; Table S1) to normalize nutrient-amended treatments to their paired control. First, we log transformed the ratio of each treatment's mean (N, P, C, NP, NPC) for each response variable (GPP, Chl  $a$ , respiration) to the mean unamended control of that variable in each stream (Burrows et al. 2017, Myrstener et al. 2018, Reisinger et al. 2016). Treatment means were used, and each NDS was not treated as a true replicate.  $\text{RR} > 0$  after log transformation indicated a positive treatment response (Table S1). We then used simple linear regression (Table S2) to investigate the relationship between autotrophic biomass (Chl  $a$ ) and productivity (GPP), as well as RR of response variables and streamwater chemistry parameters (e.g., C loss). All statistical analyses were performed in R.

### Reach-scale nutrient uptake experiments

To determine how inorganic nutrient and labile C uptake varied in streams with differing water chemistry and light conditions, we used the tracer additions for spiraling curve characterization method of slug addition for nutrient uptake experiments (Covino et al. 2010) in 2017 and 2018. We selected a reach of  $\sim 200$  m in each stream and measured stream depths and widths at 10 uniformly spaced transects along the reaches. To prepare timing for nutrient releases,

**Table 3.** Nutrient limitation of gross primary production (GPP), chlorophyll  $a$  (Chl  $a$ ), and respiration (ecosystem respiration [ER] and heterotrophic respiration [HR]). First-degree ( $1^\circ$ ) and 2<sup>nd</sup>-degree ( $2^\circ$ ) nutrient limitation of each individual stream were determined using a Type III analysis of variance following a linear mixed-effects model (equation: variable  $\sim$  treatment + shading + treatment  $\times$  shading + (1/stream)). Tukey's honestly significant difference method was used to calculate  $p$ -values of pairwise comparisons (Table S5). Effect size calculated as the mean ( $n = 20$  for ER, HR, and GPP;  $n = 36$  for Chl  $a$ ) difference between each treatment and controls across streams. Nutrient treatments were compared with unamended controls to determine the limiting resource of each stream. Effect sizes and  $p$ -values for GPP and Chl  $a$  are shown only for high-light treatments because shaded treatments were always lower than high-light treatments ( $p < 0.001$ ; Table S4, Figs 3, 4). Effect sizes and  $p$ -values for respiration are displayed for shaded and high-light treatments because high-light treatments represent ER, whereas shaded treatments include only HR. – indicates no data.

Response variable	N		P		C		NP		NPC		Resource limitation	
	Effect size	$p$	Effect size	$p$	Effect size	$p$	Effect size	$p$	Effect size	$p$	$1^\circ$ limitation	$2^\circ$ limitation
GPP	−6.28	1.00	7.11	0.99	0.36	1.00	6.61	1.00	−7.79	0.99	Light	–
Chl $a$	−0.32	0.03	0.29	0.40	−0.41	0.03	1.09	<0.001	0.58	0.03	Light	N, P
ER high light	−1.35	1.00	7.75	0.003	11.70	<0.001	11.84	<0.001	41.25	<0.001	C, P	N
HR shaded	1.97	0.04	1.41	0.10	17.75	<0.001	3.06	<0.001	41.93	<0.001	C, N	P

we measured travel time and discharge a day prior to uptake experiments by releasing a 300-g slug of NaCl and monitoring the peak in conductivity (Pro30 conductivity meter, Yellow Springs Instruments). To separate autotrophic and heterotrophic processes, we measured heterotrophic nutrient uptake in the dark and measured autotrophic and heterotrophic nutrient uptake in full sunlight. We did not alter riparian vegetation to influence stream channel light filtration during these uptake experiments. Because temperature in these streams is relatively consistent between day and night (generally  $<3^{\circ}\text{C}$  difference over 24 h; SAW, unpublished data), we assumed that stream temperature did not control respiration. We monitored PAR throughout uptake experiments to ensure difference in PAR during night and day additions (PAR logger; Odyssey®, Christchurch, New Zealand). Nutrient uptake experiments were conducted in August and September to ensure sufficient darkness for multiple uptake experiments, but variable discharge due to high precipitation during these months limited nutrient uptake experiments in 2018 to streams C1, C2, and C3.

To measure nutrient uptake, we added a slug containing a conservative tracer (NaCl) and either a single nutrient (e.g., +P) or a combination of nutrients and acetate (+NP or +NPC). Because P concentration is low in CPCRW streams and is likely limiting (Mutschlecner et al. 2017), we chose P as the only single nutrient used in uptake experiments. We measured uptake of inorganic nutrients (+P, +NP) in all 4 streams in 2017 under light conditions and uptake of inorganic nutrients and DOC (+P, +NPC) in C1, C2, and C3 in 2018 under both light and dark conditions. We were unable to visit all streams and conduct all experiments each year because of timing and resource limitations, resulting in 8 experiments in 2017 and 9 in 2018. In 2017, we conducted all nutrient uptake experiments between 10 to 25 August. In 2018, we measured nutrient uptake in C1 and C2 on 9 September and in C3 on 30 September. Uptake measurements within a single stream were conducted within 24 h to assure similar discharge throughout experimentation. We injected slugs containing nutrients as an instantaneous addition at the top of the chosen stream reach, and we sampled the break-through curve with 25 to 30 water samples collected in acid-washed HDPE bottles at the bottom of the reach. The targeted conservative tracer (NaCl) concentration was adjusted to be  $\sim 10$  mg Cl<sup>-</sup>/L above background concentration, whereas the mass of P was targeted to be 100  $\mu\text{g PO}_4^{3-}$ /L above ambient conditions (Covino et al. 2010; Table S3). We then calculated N and acetate concentrations based on the Redfield ratio and P concentration (Redfield 1958). We reduced acetate concentration as needed to ensure complete solute dissolution in slug additions (Table S3). We calculated ambient nutrient uptake length ( $S_w$ ), areal uptake rate ( $U$ ), and uptake velocity ( $V_f$ ) by using the tracer additions for spiraling curve characterization method (Covino et al. 2010). No statistical

analyses were conducted on uptake results because of inadequate sample size.

## RESULTS

### CPCRW streamwater chemistry

Streamwater chemistry varied among streams in the 2017 and 2018 field seasons but was relatively stable in each stream over the 20-d NDS incubation (Table 2). During the 2017 and 2018 field seasons, DOC concentration was highest in C3, the stream draining the catchment underlain with the highest permafrost extent, ranging from 3.6 to 4.1 mg C/L. DOC and SUVA<sub>254</sub> were both lowest at C4. In contrast, NO<sub>3</sub><sup>-</sup> was highest in C4, often exceeding 650  $\mu\text{g N/L}$ . C1 had the lowest mean NO<sub>3</sub><sup>-</sup> concentration, ranging from 302 to 332  $\mu\text{g N/L}$ . SRP concentration remained low in all study streams, rarely exceeding 4  $\mu\text{g P/L}$ , with little fluctuation among streams. Discharge varied with precipitation over field seasons but averaged 64.0 L/s in C2, 75.1 L/s in C3, and 115.3 L/s in C4 in 2018. Discharge was the most variable in C3 (Table 2). In C1 discharge was only measured once during the 2018 uptake experiments and was greater than all other streams at 173.0 L/s.

During the 2018 NDS deployment, general stream chemistry was stable. SRP concentration remained  $<6$   $\mu\text{g P/L}$  in all streams (Table 2). NO<sub>3</sub><sup>-</sup> concentration was highest in C4, ranging from 621  $\mu\text{g N/L}$  to 685  $\mu\text{g N/L}$ , and was 2 $\times$  higher than in C1, which had a mean of 260  $\mu\text{g N/L}$ . NH<sub>4</sub><sup>+</sup> concentration exhibited less variation than NO<sub>3</sub><sup>-</sup> during NDS deployment, remaining  $<40$   $\mu\text{g N/L}$  in all 4 streams. DOC concentration was variable among streams but was lowest in C4. SUVA<sub>254</sub> was also consistently lower in C4 when compared with the other 3 streams. Temperature remained below  $6^{\circ}\text{C}$  in all streams with C3 consistently the coldest stream at  $1.95^{\circ}\text{C}$ . Discharge varied over NDS incubations with precipitation. Mean discharge was highest in C4 (106.3 L/s), which was almost twice as high as mean discharge in C2 (63.0 L/s). Discharge was not measured at C1 during the NDS incubations but was relatively high when measured in conjunction with uptake experimentation.

LDOC varied across streams (Table 1). C1 and C2 had the highest % DOC loss over 40-d incubations at 10.92 and 10.21%, respectively. C3 and C4, the streams with highest and lowest DOC concentration, respectively, had  $<6\%$  C loss over 40-d incubations.

**Patch-scale response to resource additions** The fixed effects (treatment and shading) in the LMMs explained much of the variation for Chl *a*, GPP, and respiration. For Chl *a*, the fixed effects explained 83% of the variation, with fixed plus random effects (stream) explaining 90% of the variance. For GPP, the fixed effects explained 67% of the variation, with fixed plus random effects explaining 76% of

the variance. For respiration, the fixed effects explained 85% of the variation, with fixed plus random effects explaining 89% of the variance. There was a strong interaction between shading and treatment for all response variables and treatments (Table S4;  $p < 0.001$ ), suggesting that nutrient treatments affected Chl  $a$ , GPP, and respiration differently in high-light vs shaded treatments across streams.

**Autotrophic response to resource additions** High-light treatments exhibited higher GPP than shaded treatments ( $p < 0.001$  for all nutrient amendments except NPC,  $p = 0.09$ ; Fig. 3). Across streams, mean GPP ranged an order of magnitude from a minimum mean of  $3.79 \mu\text{g O}_2 \text{ cm}^{-2} \text{ h}^{-1}$  in shaded N treatments to a maximum mean of  $47.35 \mu\text{g O}_2 \text{ cm}^{-2} \text{ h}^{-1}$  in high-light P treatments. GPP did not vary with nutrient additions when compared across streams in high light ( $p > 0.99$  for all nutrient amendments; Table 3, Fig. 3).

Autotrophic biomass, like GPP, responded positively to light availability. Across streams, Chl  $a$  was consistently lower in shaded treatments than high-light treatments ( $p < 0.001$  for all nutrient amendments; Table S4, Fig. 4). Unlike GPP, Chl  $a$  exhibited a larger positive response to nutrient additions under high light. In single nutrient additions under high light, Chl  $a$  was slightly elevated in treatments containing P with a mean of  $1.51 \mu\text{g/cm}^2$ , but was

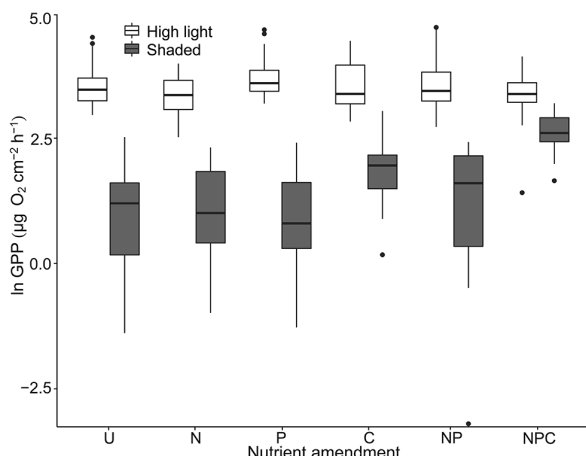


Figure 3. Gross primary production (GPP) of biofilms colonized during instream nutrient diffusing substrata deployments across study streams in the Caribou-Poker Creeks Research Watershed in central Alaska, USA. GPP values are transformed by the natural log. Nutrient amendments include unamended control (U), ammonium (N), phosphorus (P), acetate (C), and combinations of these (NP, NPC). White boxes correspond to high-light treatments, and gray boxes correspond to shaded treatments. The center lines, box extent, error bars, and points indicate the 50<sup>th</sup> percentile (median), the 25<sup>th</sup> and 75<sup>th</sup> percentile (interquartile range), the 95% CIs, and outliers, respectively.

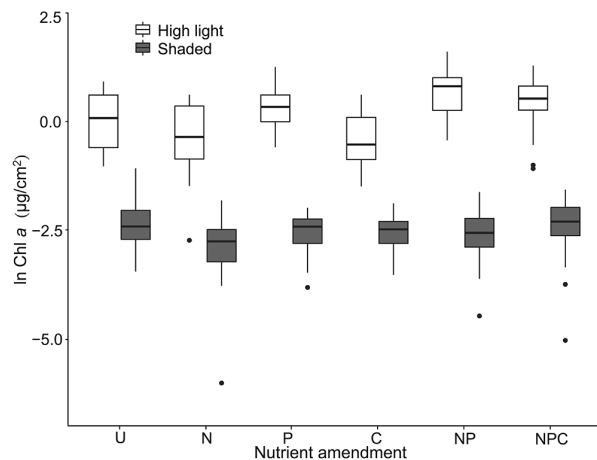


Figure 4. Chlorophyll  $a$  (Chl  $a$ ) quantified from biofilms colonized during instream nutrient diffusing substrata deployments across study streams in the Caribou-Poker Creeks Research Watershed in central Alaska, USA. Chl  $a$  values are transformed by the natural log. Nutrient amendments include unamended control (U), ammonium (N), phosphorus (P), acetate (C), and combinations of these (NP, NPC). White boxes correspond to high-light treatments, and gray boxes correspond to shaded treatments. The center lines, box extent, error bars, and points indicate the 50<sup>th</sup> percentile (median), the 25<sup>th</sup> and 75<sup>th</sup> percentile (interquartile range), the 95% CIs, and outliers, respectively.

highest in NP treatments with a mean of  $2.31 \mu\text{g/cm}^2$ , representing biomass twice as high as unamended controls ( $1.22 \mu\text{g/cm}^2$ ;  $p < 0.001$ ; Table 3). Across streams, algal growth under high light was suppressed in treatments containing acetate alone and N alone (effect size =  $-0.41$  and  $-0.32$ , respectively;  $p = 0.03$ ; Table 3, Fig. 4). Similar to GPP, Chl  $a$  accumulation under high light was lower in NPC treatments ( $1.80 \mu\text{g/cm}^2$ ) than NP treatments. High-light treatments amended with P contained more biomass accumulation than treatments with N ( $p < 0.001$ ) and C ( $p < 0.001$ ), but these P-amended treatments were not substantially higher than unamended controls ( $p = 0.40$ ; Fig. 4).

We calculated GPP RR to normalize nutrient-amended treatments to their paired controls and looked for correlations between autotrophic biomass and productivity and stream physicochemical parameters. RR<sub>P</sub> was the only treatment that had a positive GPP response in all streams when compared with mean unamended controls (Table S1). For Chl  $a$ , RR<sub>NP</sub> and RR<sub>NPC</sub> showed similar positive responses, and RR<sub>P</sub> was  $<0$  in only 1 stream. Autotrophic biomass (Chl  $a$ ) and GPP were positively correlated (linear regression:  $r^2 = 0.63$ ,  $p < 0.001$ ; Fig. S1). We did not find any strong correlations between ambient nutrient concentrations, LDOC, permafrost extent, and RR of any nutrient amendment for autotrophic biomass or productivity across streams (Table S2).

**Heterotrophic response to resource additions** In shaded treatments, HR increased following acetate and inorganic nutrient addition (Table 3, Fig. 5). This positive HR response was strong in treatments containing N (effect size = 1.97,  $p = 0.04$ ), C (17.75,  $p < 0.001$ ), NP (3.06,  $p < 0.001$ ), and NPC (41.93,  $p < 0.001$ ). Under high light in treatments containing C, ER was only slightly higher than HR, (29.83 and 22.02  $\mu\text{g O}_2 \text{ cm}^{-2} \text{ h}^{-1}$ , respectively) but still greater than unamended high-light controls (18.13  $\mu\text{g O}_2 \text{ cm}^{-2} \text{ h}^{-1}$ ). ER rates slightly increased in high-light treatments with just inorganic P or acetate but were highest in treatments containing combinations of inorganic N, P, and acetate (effect size = 41.25,  $p < 0.001$ ; Table 3, Fig. 5). In contrast, ER rates under high light did not differ from the control when inorganic N was the sole nutrient amendment, with mean ER actually slightly lower (18.13 to 16.78  $\mu\text{g O}_2 \text{ cm}^{-2} \text{ h}^{-1}$ ; effect size = -1.35). Treatments with acetate (alone and combined with inorganic nutrients) were more similar between shaded and high-light treatments than treatments amended with just inorganic nutrients. GPP:ER was  $>1$  in most high-light treatments (Fig. 6) except with acetate addition. In general, shaded treatment GPP:HR was  $<1$ , except in unamended controls and P-amended treatments. In high light, all ER RR were weakly positively correlated with C loss over time ( $r^2 =$

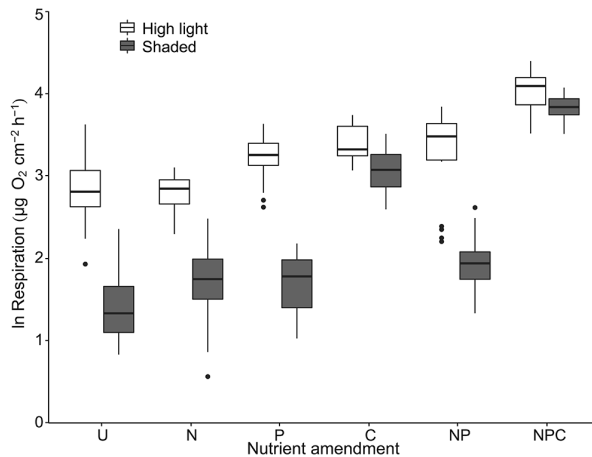


Figure 5. Respiration quantified from biofilms colonized during instream nutrient diffusing substrata deployments across study streams in the Caribou-Poker Creeks Research Watershed in central Alaska, USA. Respiration values are transformed by the natural log. High-light treatments represent ecosystem respiration, whereas shaded treatments represent heterotrophic respiration. Nutrient amendments include unamended control (U), ammonium (N), phosphorus (P), acetate (C), and combinations of these (NP, NPC). White boxes correspond to high-light treatments, and gray boxes correspond to shaded treatments. The center lines, box extent, error bars, and points indicate the 50<sup>th</sup> percentile (median), the 25<sup>th</sup> and 75<sup>th</sup> percentile (interquartile range), the 95% CIs, and outliers, respectively.

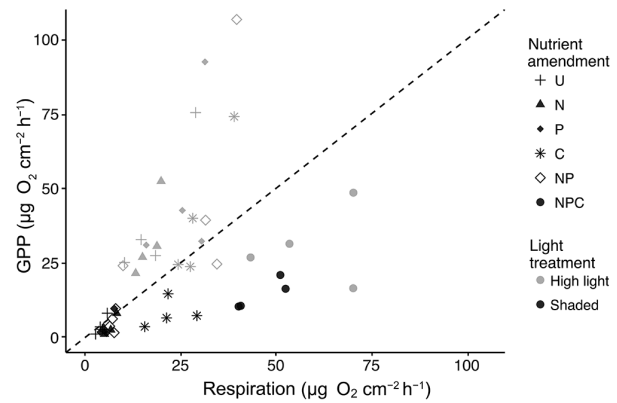


Figure 6. Gross primary production (GPP) and respiration of biofilms colonized on nutrient diffusing substrata fritted glass filter disks across all streams and treatments. Light gray points represent high-light treatment means in each stream ( $n = 5$ ), and black points represent shaded treatment means in each stream ( $n = 5$ ). Shapes represent nutrient treatments. 1:1 ratio of GPP to respiration (ecosystem respiration and heterotrophic respiration) is represented by the dashed line.

0.12–0.82,  $p = 0.66$ –0.09; Fig. 7). All HR RR responded positively to nutrient amendment ( $\text{RR} > 0$ ), but treatments containing C were elevated compared with treatments with inorganic nutrients alone (Table S1).

### Reach-scale nutrient uptake

Nutrient uptake varied among streams and appeared to be affected by both nutrient amendment and light availability (Table 4). In 2017 in both C2 and C3, daytime NP-uptake amendments had P ambient uptake length ( $S_w$ ; m) measuring  $\frac{1}{2}$  as long as amendments including P alone. When P was the sole nutrient added, P  $S_w$  varied with light treatment but was similar across headwater streams and years. Daytime P  $S_w$  varied from 344 to 557 m in 2018, whereas the single detectable nighttime treatment was ~twice as long (1086 m). In 2018, adding  $\text{NH}_4^+$  and acetate did not decrease P  $S_w$  regardless of light treatment. Under dark conditions, P  $S_w$  was not detectable in C2, regardless of nutrient addition (both P and NPC treatments).  $\text{NH}_4^+$  and acetate  $S_w$  were not detectable in the study streams during the additions. Measurements of ambient uptake velocity ( $V_f$ ; mm/min) and areal uptake ( $U$ ;  $\mu\text{g P m}^{-2} \text{ min}^{-1}$ ) varied among years and light treatments but did not show predictable patterns (Table 4). Additional experiments with greater replication are needed.

## DISCUSSION

### Nutrient limitation in boreal streams

Using patch- and reach-scale approaches, we examined how variation in water chemistry affects competition

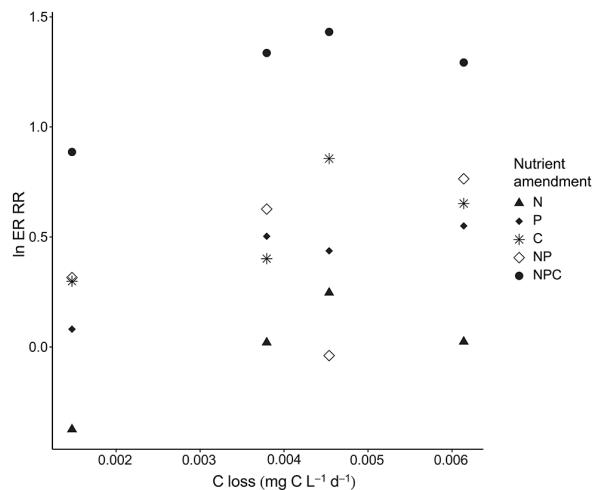


Figure 7. Relationship between mean ecosystem respiration (ER) response ratios (RR) and C loss ( $\text{mg C L}^{-1} \text{d}^{-1}$ ). Plot includes data for mean nutrient amendment for high-light nutrient diffusing substrata ( $n = 5$ ) in all streams plotted against mean loss of C ( $n = 8$ ) over 40-d labile dissolved organic C incubations. Nutrient amendments include ammonium (N), phosphorus (P), acetate (C), and combinations of these (NP, NPC). Shapes represent ER RR by nutrient treatment (Table S2; simple linear regression:  $\text{RR}_N: r^2 = 0.55, p = 0.25$ ;  $\text{RR}_P: r^2 = 0.82, p = 0.09$ ;  $\text{RR}_C: r^2 = 0.51, p = 0.28$ ;  $\text{RR}_{NP}: r^2 = 0.12, p = 0.66$ ;  $\text{RR}_{NPC}: r^2 = 0.60, p = 0.22$ ).

between autotrophs and heterotrophs in boreal headwater streams under high-light and shaded conditions. Our research objectives were to determine which nutrient and energy resources control autotrophic and heterotrophic activity and biomass in streams of varying permafrost influence and how these resources affect competition for inorganic nutrients between autotrophs and heterotrophs in these streams. Our prediction that microbial growth and productivity are primarily P limited was not supported, and we found that biomass and productivity of autotrophs and heterotrophs were largely constrained by a combination of resources at the patch and reach scales. Our results did support our prediction that heterotrophs might be outcompeting autotrophs for nutrients in the presence of labile C.

At both scales, a combination of resources limited both autotrophs and heterotrophs. At the patch scale, HR was primarily limited by C and P availability and secondarily limited by inorganic N, whereas ER was primarily limited by C and N availability and secondarily limited by inorganic P. This result illustrates that primarily organic C controlled HR and nutrient assimilation by heterotrophs (Robbins et al. 2017). Autotrophic biomass and productivity, however, were both primarily light limited, and only autotrophic biomass was secondarily colimited by N and

P (Table 3). Therefore, light, in combination with inorganic nutrients, controlled autotrophic biomass accrual and productivity (Bernhardt and Likens 2004). This co-limitation of microbial processes is common and occurs when there is simultaneous biological demand for multiple resources for microbial growth and productivity (Warren et al. 2017).

With such low concentrations of P in CPCRW streams, it is surprising that P alone was not found to be primarily limiting of autotrophic or heterotrophic growth or productivity. P limitation is common in Alaskan and other high-latitude headwater streams (Peterson et al. 1985, Corning et al. 1989, Diemer et al. 2015), although N limitation also occurs (Burrows et al. 2015, Myrstener et al. 2018). The finding that N and P were not solely primarily limiting across the CPCRW suggests that elevated nutrient concentrations might not be the most important drivers of autotrophic and heterotrophic processes in the CPCRW (Huryn et al. 2014).

#### Patch-scale resource limitation of autotrophs

Light was the primary control of autotrophic productivity and biomass accrual on NDS in CPCRW streams (Table 3, Fig. 4). Nutrients also played a role in autotrophic biomass, with increased Chl  $\alpha$  in treatments containing both inorganic N and P (Fig. 4). GPP, however, was not substantially limited by nutrients (Table 3, Fig. 3) but measured 15 to 25% higher in treatments containing P than unamended or N-only treatments (Fig. 3). This trend, as well as our finding that NP increases Chl  $\alpha$  accumulation, suggests that nutrients, in addition to light, are indeed important drivers of autotrophic productivity in streams of the CPCRW, a common finding among studies utilizing NDS in other stream networks (Tank and Dodds 2003, Johnson et al. 2009b, Reisinger et al. 2016, Myrstener et al. 2018).

#### Patch-scale resource limitation of heterotrophs

Similar to autotrophs, heterotrophs can be highly responsive to resource gradients (Van Horn et al. 2011, Myrstener et al. 2018). Our results suggest that HR in CPCRW streams is regulated by both labile C and inorganic nutrients (Table 3, Fig. 5) and that the uptake of these resources is tightly coupled. HR responded positively to inorganic nutrient addition alone, yet responses increased by 100% when inorganic nutrients were introduced in combination with a labile C source (Table 3, Fig. 5). This suggests that C limitation needed to be alleviated before heterotrophs can utilize N and P. In high-light treatments, there were similar patterns of increased ER in treatments containing labile C and inorganic nutrients, but ER rates across streams were consistently higher than HR across nutrient treatments (Fig. S1). This persistent C limitation of respiration (both ER and HR) could be driven by a relatively recalcitrant C pool (Balcarczyk et al. 2009, Mutschlechner et al.

Table 4. P uptake parameters calculated using the tracer additions for spiraling curve characterization method (Covino et al. 2010). All nutrient uptake experimentation was completed during August and September 2017 (light) and 2018 (light and dark). Uptake parameters are ambient nutrient uptake length ( $S_w$ ), areal uptake rate ( $U$ ), and uptake velocity ( $V_f$ ). Nutrient amendments include phosphorous (+P), ammonium (N) and P (+NP), and N, P, and acetate (+NPC). – represents where uptake experiments were not performed, ND indicates no detectable uptake.

Year	Nutrient amendment	Shading effect	Stream	$S_w$ (m)	$U$ ( $\mu\text{g P m}^{-2} \text{min}^{-1}$ )	$V_f$ (mm/min)
2017	+P	Light	C1	417.5	18.7	8.8
			C2	502.4	13.3	5.3
			C3	1419.9	3.1	2.2
			C4	ND	ND	ND
	+NP	Light	C1	646.8	18.8	5.7
			C2	263.1	26.7	10.1
			C3	578.1	14.0	5.4
			C4	454.0	34.3	6.9
2018	+P	Light	C1	343.7	42.9	27.8
			C2	447.0	27.6	12.8
			C3	557.1	20.2	10.0
			C4	–	–	–
	+P	Dark	C1	–	–	–
			C2	ND	ND	ND
			C3	1085.6	13.1	5.1
			C4	–	–	–
	+NPC	Light	C1	–	–	–
			C2	1077.1	9.7	5.3
			C3	554.5	34.1	10.0
			C4	–	–	–
	+NPC	Dark	C1	–	–	–
			C2	ND	ND	ND
			C3	1073.7	11.7	5.2
			C4	–	–	–

2018), which limits microbial decomposition of molecularly complex organic matter in these streams.

We also found that RR for ER were positively correlated to C loss over time (Fig. 7) in high-light treatments, regardless of nutrient amendment. Although this trend was not statistically strong, it suggests that nutrient use efficiency increases with C lability, a finding well supported in the literature (Ardón and Pringle 2007, Johnson et al. 2012). These results reiterate the importance of both inorganic nutrients and labile organic C in combination for heterotrophic growth, whether derived through autochthonous or allochthonous pathways (Rier and Stevenson 2002). Although we did not find any direct relationships with heterotrophic productivity and permafrost cover, this positive relationship between ER and C loss suggests that increased C lability with permafrost loss could be linked to increased heterotrophic productivity under conditions of increased nutrient export in these headwater streams (Balcarczyk et al. 2009).

### Reach-scale resource limitation

Whereas autotrophic and heterotrophic nutrient assimilation at the patch-scale was limited by various combinations of resources, uptake at the reach-scale appeared to be largely affected by light and inorganic nutrients (Table 4). This result suggests that autotrophs predominately contributed to nutrient uptake in a given stream reach, and organic C available to heterotrophs did not impact P uptake (see next paragraph). This finding was surprising, considering that most headwater streams are net heterotrophic (Vannote et al. 1980), with riparian vegetation suppressing algal growth and with rates of  $HR > GPP$ . At the patch scale, GPP exceeded ER in unamended biofilms colonized under high-light conditions, suggesting that biofilms exposed to full sunlight in the CPCRW may be autotroph dominated (Fig. 6). Alternatively, this finding could be attributed to the removal of riparian vegetation around NDS, allowing increased sunlight penetration to the streambed, and the use of inorganic substrata (fritted glass filter disks)

for biofilm colonization, both which may select for colonization of microbial biofilms dominated by autotrophs (Johnson et al. 2009b).

Increased labile C supply can alleviate nutrient limitation and, therefore, increase nutrient uptake by stream heterotrophs (Johnson et al. 2009a, Blaen et al. 2014, Docherty et al. 2018). We did not find evidence that acetate in conjunction with nutrient additions increased uptake of P under ambient light conditions (Table 4), but previous findings suggest that P and C uptake are coupled in streams of the CPCRW (Mutschlecner et al. 2017). Under dark experimental conditions, acetate addition also did not appear to enhance P uptake. Because we added C as labile acetate, we did not expect C uptake to be unmeasurable in conditions favoring heterotrophs. The lack of observable C uptake suggests that P limitation and N limitation may not have been sufficiently alleviated during experimentation or that there was P retention through abiotic mechanisms, such as physical sorption (Schade et al. 2016). The difference between P uptake length during light and dark experimentation, however, makes adsorption in the substrate seem unlikely. Finding dissimilar resource limitation at the patch and reach scale can occur (Docherty et al. 2018, Tromboni et al. 2018) and suggests that only focusing on 1 scale, both spatially and temporally, may be misleading.

### Competition driven by labile C

Autotrophs and heterotrophs rely on inorganic nutrients for GPP and ER (Battin et al. 2016) and, therefore, compete within biofilms for these nutrients (Currie 1990). In the study streams, unamended treatment biofilms were autotrophic ( $GPP > ER$ ) under high-light conditions, but heterotrophic ( $GPP < HR$ ) in shaded treatments (Fig. 6). When a labile C source was introduced, however, ER and HR increased to exceed GPP on unamended controls regardless of shading effect, suggesting heterotrophic uptake of C and increased competition for inorganic nutrients.

Competition between autotrophs and heterotrophs for inorganic nutrients was evidenced in the suppression of autotrophic response to nutrient enrichment. Both GPP and Chl  $\alpha$  were lower when nutrient amendments included organic C in addition to inorganic nutrients (NPC) vs without C (NP) in most streams (Figs S3, S4). Because autotrophs cannot derive energy from organic C, Chl  $\alpha$  should not be affected by organic C availability in addition to inorganic nutrients. The corresponding observed decrease in GPP suggests that heterotrophs may be outcompeting autotrophs for inorganic nutrients with the addition of labile C. Similarly, competition for nutrients between autotrophs and heterotrophs was further evidenced by lower algal biomass with the addition of acetate (Chl  $\alpha$  lower in NPC than NP treatments and lower in C treatments than control; Fig. S3), a finding supported by the literature (Joint et al. 2002, Stets and Cotner 2008, Bechtold et al. 2012).

### Resource limitation of biofilms in a changing boreal forest

In boreal forest streams of Sweden and tundra streams of Greenland underlain by continuous permafrost, both autotrophic and heterotrophic biofilms have been found to be persistently N limited at the patch scale (Burrows et al. 2015, Docherty et al. 2018, Myrstener et al. 2018). This N limitation often exists in conjunction with other resource limitation, especially light and C (Burrows et al. 2017, Myrstener et al. 2018). Streams in Arctic and subarctic Alaska, however, are more commonly P limited (Peterson et al. 1986, Slavik et al. 2004, Mutschlecner et al. 2017). Studies conducted in the Kuparuk river and subarctic Alaskan headwater streams suggest resource colimitation (Mutschlecner et al. 2017), highlighting the importance of autochthonous C to heterotrophic biofilm functioning (Peterson et al. 1986) as suggested in our patch-scale research at the CPCRW.

As climate change reshapes regions with permafrost and as high-latitude watersheds warm, nutrient use in stream biofilm communities will change. Increases in nutrient and C pools (Frey et al. 2007a, Reyes and Lougheed 2015), coupled with warming soils, will likely lead to increased stream productivity. Our results indicate that boreal forest stream biofilms will become more productive with these increases in nutrient and C pools, yet heterotrophs may outcompete autotrophs in the presence of labile C. This labile C will then mobilize into stream networks (Balcarczyk et al. 2009, Abbott et al. 2014) as the large C pools locked within this frozen ground are released through permafrost degradation (Zimov et al. 2006). Once mobilized, this labile C will likely be utilized through increased heterotrophic microbial decomposition and released as CO<sub>2</sub> (Vonk et al. 2015), further contributing to permafrost–climate feedbacks (Schuur et al. 2015). As permafrost thaws and permafrost active layer depth increases, rising stream temperature will positively affect autotrophic nutrient use efficiency (Cross et al. 2005) and primary production rates (Hood et al. 2018). These changes will also affect instream nutrient use and retention, altering biofilm function and nutrient export downstream. Further unraveling the complexity of resource use by, and availability to, stream autotrophs and heterotrophs will allow us to predict how headwater stream ecosystems will respond to changes in climate and, ultimately, permafrost loss in the boreal forest.

### ACKNOWLEDGEMENTS

Author contributions: SAW and JBJ conceived and designed this research study. SAW collected, analyzed, and interpreted the data with oversight from JBJ. SAW and JBJ wrote the paper.

This project was funded through the Bonanza Creek Long Term Ecological Research program (National Science Foundation grant DEB-1636476) and by the United States Department of Agriculture Forest Service, Pacific Northwest Research Station (RJVA-PNW-01-JV-11261952-231). Additional funding was

provided by the University of Alaska Fairbanks and the Institute of Arctic Biology. We thank Audrey Mutschlechner, Marie Schmidt, and Rachel Voight for assistance in the field, and Christina Baker for help in the laboratory. We would also like to acknowledge Dr Mary Beth Leigh, Dr Roger Reuss, and Dr Diane Wagner for help with project development, study design, and for providing feedback on this manuscript. We thank Dr Tamara Harms for the use of lab analyzers.

## LITERATURE CITED

Abbott, B. W., J. R. Larouche, J. B. Jones Jr, W. B. Bowden, and A. W. Balser. 2014. Elevated dissolved organic carbon biodegradability from thawing and collapsing permafrost. *Journal of Geophysical Research: Biogeosciences* 119:2049–2063.

Ardón, M., and C. M. Pringle. 2007. The quality of organic matter mediates the response of heterotrophic biofilms to phosphorus enrichment of the water column and substratum. *Freshwater Biology* 52:1762–1772.

Balcarczyk, K. L., J. B. Jones Jr, R. Jaffé, and N. Maie. 2009. Stream dissolved organic matter bioavailability and composition in watersheds underlain with discontinuous permafrost. *Biogeochemistry* 94:255–270.

Bates, D., M. Maechler, B. M. Bolker, and S. Walker. 2015. Fitting linear mixed-effects models using *lme4*. *Journal of Statistical Software* 67:1–48.

Battin, T. J., K. Besemer, M. M. Bengtsson, A. M. Romani, and A. I. Packmann. 2016. The ecology and biogeochemistry of stream biofilms. *Nature Reviews Microbiology* 14:251–263.

Battin, T. J., L. A. Kaplan, S. Findlay, C. S. Hopkinson, E. Marti, and A. I. Packman. 2008. Biophysical controls on organic carbon fluxes in fluvial networks. *Nature Geoscience* 1:95–100.

Bechtold, H. A., A. M. Marcarelli, C. V. Baxter, and R. S. Inouye. 2012. Effects of N, P, and organic carbon on stream biofilm nutrient limitation and uptake in a semi-arid watershed. *Limnology and Oceanography* 57:1544–1554.

Bernhardt, E. S., and G. E. Likens. 2002. Dissolved organic carbon enrichment alters nitrogen dynamics in a forest stream. *Ecology* 83:1689–1700.

Bernhardt, E. S., and G. E. Likens. 2004. Controls on periphyton biomass in heterotrophic streams. *Freshwater Biology* 49:14–27.

Blaen, P. J., A. M. Milner, D. M. Hannah, J. E. Brittain, and L. E. Brown. 2014. Impact of changing hydrology on nutrient uptake in high arctic rivers. *River Research and Applications* 30:1073–1083.

Burrows, R. M., E. R. Hotchkiss, M. Jonsson, H. Laudon, B. G. McKie, and R. A. Sponseller. 2015. Nitrogen limitation of heterotrophic biofilms in boreal streams. *Freshwater Biology* 60: 1237–1251.

Burrows, R. M., H. Laudon, B. G. McKie, and R. A. Sponseller. 2017. Seasonal resource limitation of heterotrophic biofilms in boreal streams. *Limnology and Oceanography* 62:164–176.

Corning, K. E., H. C. Duthie, and B. J. Paul. 1989. Phosphorus and glucose uptake by seston and epilithon in boreal forest streams. *Journal of North American Benthological Society* 8: 123–133.

Covino, T. P., B. L. McGlynn, and R. A. McNamara. 2010. Tracer Additions for Spiraling Curve Characterization (TASCC): Quantifying stream nutrient uptake kinetics from ambient to saturation. *Limnology and Oceanography: Methods* 8: 484–498.

Cross, W. F., J. P. Benstead, P. C. Frost, and S. A. Thomas. 2005. Ecological stoichiometry in freshwater benthic systems: Recent progress and perspectives. *Freshwater Biology* 50:1895–1912.

Cross, W. F., J. M. Hood, J. P. Benstead, A. D. Huryn, and D. Nelson. 2015. Interactions between temperature and nutrients across levels of ecological organization. *Global Change Biology* 21:1025–1040.

Currie, D. J. 1990. Large-scale variability and interactions among phytoplankton, bacterioplankton, and phosphorus. *American Society of Limnology and Oceanography* 35:1437–1455.

Davidson, E. A., and I. A. Janssens. 2006. Temperature sensitivity of soil carbon decomposition and feedbacks to climate change. *Nature* 440:165–173.

Demars, B. O., J. R. Manson, J. S. Olafsson, G. M. Gislason, R. Gudmundsdottir, G. U. Y. Woodward, J. Reiss, D. E. Pichler, J. J. Rasmussen, and N. Friberg. 2011. Temperature and the metabolic balance of streams. *Freshwater Biology* 56:1106–1121.

Diemer, L. A., W. H. McDowell, A. S. Wymore, and A. S. Prokushkin. 2015. Nutrient uptake along a fire gradient in boreal streams of central Siberia. *Freshwater Science* 34:1443–1456.

Docherty, C. L., T. Riis, D. M. Hannah, S. R. Leth, and A. M. Milner. 2018. Nutrient uptake controls and limitation dynamics in north-east Greenland streams. *Polar Research* 37:1–12.

Dodds, W. K. 2007. Trophic state, eutrophication and nutrient criteria in streams. *Trends in Ecology and Evolution* 22:669–676.

Elser, J. J., M. E. Bracken, E. E. Cleland, D. S. Gruner, W. S. Harpole, H. Hillebrand, J. T. Ngai, E. W. Seabloom, J. B. Shurin, and J. E. Smith. 2007. Global analysis of nitrogen and phosphorus limitation of primary producers in freshwater, marine and terrestrial ecosystems. *Ecology Letters* 10: 1135–1142.

Frey, K. E., and J. W. McClelland. 2009. Impacts of permafrost degradation on arctic river biogeochemistry. *Hydrological Processes* 23:169–182.

Frey, K. E., J. W. McClelland, R. M. Holmes, and L. C. Smith. 2007a. Impacts of climate warming and permafrost thaw on the riverine transport of nitrogen and phosphorus to the Kara Sea. *Journal of Geophysical Research: Biogeosciences* 112:1–10.

Frey, K. E., D. I. Siegel, and L. C. Smith. 2007b. Geochemistry of west Siberian streams and their potential response to permafrost degradation. *Water Resources Research* 43:WR004902.

Hill, W. R., S. E. Fanta, and B. J. Roberts. 2009. Quantifying phosphorus and light effects in stream algae. *Limnology and Oceanography* 54:368–380.

Hinzman, L. D., N. D. Bettez, W. R. Bolton, F. S. Chapin, M. B. Dyurgerov, C. L. Fastie, B. Griffith, R. D. Hollister, A. Hope, H. P. Huntington, A. M. Jensen, G. J. Jia, T. Jorgenson, D. L. Kane, D. R. Klein, G. Kofinas, A. H. Lynch, A. H. Lloyd, A. D. McGuire, F. E. Nelson, W. C. Oechel, T. E. Osterkamp, C. H. Racine, V. E. Romanovsky, R. S. Stone, D. A. Stow, M. Sturm, C. E. Tweedie, G. L. Vourlitis, M. D. Walker, D. A.

Walker, P. J. Webber, J. M. Welker, K. S. Winker, and K. Yoshikawa. 2005. Evidence and implications of recent climate change in northern Alaska and other Arctic regions. *Climatic Change* 72:251–298.

Hood, J. M., J. P. Benstead, W. F. Cross, A. D. Huryn, P. W. Johnson, G. M. Gislason, J. R. Junker, D. Nelson, J. S. Olafsson, and C. Tran. 2018. Increased resource use efficiency amplifies positive response of aquatic primary production to experimental warming. *Global Change Biology* 24:1069–1084.

Huryn, A. D., J. P. Benstead, and S. M. Parker. 2014. Seasonal changes in light availability modify the temperature dependence of ecosystem metabolism in an arctic stream. *Ecology* 95:2826–2839.

Johnson, L. T., T. V. Royer, J. M. Edgerton, and L. G. Leff. 2012. Manipulation of the dissolved organic carbon pool in an agricultural stream: Responses in microbial community structure, denitrification, and assimilatory nitrogen uptake. *Ecosystems* 15:1027–1038.

Johnson, L. T., J. L. Tank, and C. P. Arango. 2009a. The effect of land use on dissolved organic carbon and nitrogen uptake in streams. *Freshwater Biology* 54:2335–2350.

Johnson, L. T., J. L. Tank, and W. K. Dodds. 2009b. The influence of land use on stream biofilm nutrient limitation across eight North American ecoregions. *Canadian Journal of Fisheries and Aquatic Sciences* 66:1081–1094.

Joint, I., P. Henriksen, G. A. Fonnes, D. Bourne, T. F. Thingstad, and B. Riemann. 2002. Competition for inorganic nutrients between phytoplankton and bacterioplankton in nutrient manipulated mesocosms. *Aquatic Microbial Ecology* 29:145–159.

Jones Jr, J. B., K. C. Petrone, J. C. Finlay, L. D. Hinzman, and W. R. Bolton. 2005. Nitrogen loss from watersheds of interior Alaska underlain with discontinuous permafrost. *Geophysical Research Letters* 32:1–4.

Kaplan, L. A., T. N. Wiegner, J. D. Newbold, P. H. Ostrom, and H. Gandhi. 2008. Untangling the complex issue of dissolved organic carbon uptake: A stable isotope approach. *Freshwater Biology* 53:855–864.

Kokelj, S. V., and M. T. Jorgenson. 2013. Advances in thermokarst research. *Permafrost and Periglacial Processes* 24:108–119.

Kuznetsova, A., P. B. Brockhoff, R. H. B. Christensen, and S. B. Jensen. 2020. *lmerTest*: Tests in linear mixed effects models. (Available from: <https://cran.r-project.org/web/packages/lmerTest/index.html>)

McDowell, W. H., A. Zsolnay, J. A. Aitkenhead-Peterson, E. G. Gregorich, D. L. Jones, D. Jödemann, K. Kalbitz, B. Marschner, and D. Schwesig. 2006. A comparison of methods to determine the biodegradable dissolved organic carbon from different terrestrial sources. *Soil Biology and Biochemistry* 38:1933–1942.

Merriam, J. L., W. H. McDowell, and W. S. Currie. 1996. A high-temperature catalytic oxidation technique for determining total dissolved nitrogen. *Soil Science Society of America Journal* 60:1050–1055.

Murphy, J., and J. P. Riley. 1962. A modified single solution method for the determination of phosphate in natural waters. *Analytica Chemica Acta* 1:31–36.

Mutschlecner, A. E., J. J. Guerard, J. B. Jones, and T. K. Harms. 2017. Phosphorus enhances uptake of dissolved organic matter in boreal streams. *Ecosystems* 21:675–688.

Mutschlecner, A. E., J. J. Guerard, J. B. Jones, and T. K. Harms. 2018. Regional and intra-annual stability of dissolved organic matter composition and biolability in high-latitude Alaskan rivers. *Limnology and Oceanography* 63:1605–1621.

Myrstener, M., G. Rocher-Ros, R. M. Burrows, A. K. Bergstrom, R. Giesler, and R. A. Sponseller. 2018. Persistent nitrogen limitation of stream biofilm communities along climate gradients in the Arctic. *Global Change Biology* 24:3680–3691.

Peterson, B. J., J. E. Hobbie, and T. L. Corliss. 1986. Carbon flow in a tundra stream ecosystem. *Canadian Journal of Fisheries and Aquatic Sciences* 43:1259–1270.

Peterson, B. J., J. E. Hobbie, M. A. Lock, T. E. Ford, J. R. Vestal, V. L. McKinley, M. A. J. Hullar, M. C. Miller, R. M. Ventullo, and G. S. Volk. 1985. Transformation of a tundra river from heterotrophy to autotrophy by addition of phosphorus. *Science* 229:1383–1386.

Peterson, B. J., R. M. Holmes, J. W. McClelland, C. J. Vorosmarty, R. B. Lammers, A. I. Shiklomanov, I. A. Shiklomanov, and S. Rahmstorf. 2002. Increasing river discharge to the Arctic Ocean. *Science* 298:2171–2173.

Petrone, K. C., J. B. Jones, L. D. Hinzman, and R. D. Boone. 2006. Seasonal export of carbon, nitrogen, and major solutes from Alaskan catchments with discontinuous permafrost. *Journal of Geophysical Research: Biogeosciences* 111:55.

Piper, L., W. F. Cross, and B. L. McGlynn. 2017. Colimitation and the coupling of N and P uptake kinetics in oligotrophic mountain streams. *Biogeochemistry* 132:165–184.

Redfield, A. C. 1958. The biological control of chemical factors in the environment. *American Scientist* 46:205–221.

Reisinger, A. J., J. L. Tank, and M. M. Dee. 2016. Regional and seasonal variation in nutrient limitation of river biofilms. *Freshwater Science* 35:474–489.

Reyes, F. R., and V. L. Lougheed. 2015. Rapid nutrient release from permafrost thaw in Arctic aquatic ecosystems. *Arctic, Antarctic, and Alpine Research* 47:35–48.

Rier, S. T., and R. J. Stevenson. 2002. Effects of light, dissolved organic carbon, and inorganic nutrients on the relationship between algae and heterotrophic bacteria in stream periphyton. *Hydrobiologia* 489:179–184.

Robbins, C. J., R. S. King, A. D. Yeager, C. M. Walker, J. A. Back, R. D. Doyle, and D. F. Whigham. 2017. Low-level addition of dissolved organic carbon increases basal ecosystem function in a boreal headwater stream. *Ecosphere* 8:e01739.

Romani, A. M., and S. Sabater. 2001. Structure and activity of rock and sand biofilms in a mediterranean stream. *Ecology* 82:3232–3245.

Schade, J. D., K. MacNeill, S. A. Thomas, C. F. McNeely, J. R. Welter, J. Hood, M. Goodrich, M. E. Power, and J. C. Finlay. 2011. The stoichiometry of nitrogen and phosphorus spiraling in heterotrophic and autotrophic streams. *Freshwater Biology* 56:424–436.

Schade, J. D., E. C. Seybold, T. Drake, S. Spawn, W. V. Sobczak, K. E. Frey, R. M. Holmes, and N. Zimov. 2016. Variation in summer nitrogen and phosphorus uptake among Siberian headwater streams. *Polar Research* 35:24571.

Schuur, E. A., A. D. McGuire, C. Schadel, G. Grosse, J. W. Harden, D. J. Hayes, G. Hugelius, C. D. Koven, P. Kuhry, D. M. Lawrence, S. M. Natali, D. Olefeldt, V. E. Romanovsky, K. Schaefer, M. R. Turetsky, C. C. Treat, and J. E. Vonk. 2015.

Climate change and the permafrost carbon feedback. *Nature* 520:171–179.

Slavik, K., B. J. Peterson, L. A. Deegan, W. B. Bowden, A. E. Hershey, and J. E. Hobbie. 2004. Long-term responses of the Kaparuk River ecosystem to phosphorus fertilization. *Ecology* 85:939–954.

Solorzano, L. 1968. Determination of ammonia in natural waters by the phenohypochlorite method. *Limnology and Oceanography* 14:799–801.

Steinman, A. D., G. A. Lamberti, and P. R. Leavitt. 2011. Biomass and pigments of benthic algae. Pages 223–241 in F. R. Hauer and G. A. Lamberti (editors). *Methods in stream ecology*. Academic Press, San Diego, California.

Sternert, R. W., J. Clasen, W. Lampert, and T. Weisse. 1998. Carbon:phosphorus stoichiometry and food chain production. *Ecology Letters* 1:146–150.

Stets, E. G., and J. B. Cotner. 2008. The influence of dissolved organic carbon on bacterial phosphorus uptake and bacterial phytoplankton in two Minnesota lakes. *Limnology and Oceanography* 53:137–147.

Tank, J. L., M. J. Bernot, and E. J. Rosi-Marshall. 2011. Nitrogen limitation and uptake. Pages 213–238 in F. R. Hauer and G. A. Lamberti (editors). *Methods in stream ecology*. Academic Press, San Diego, California.

Tank, J. L., and W. K. Dodds. 2003. Nutrient limitation of epilithic and epixylic biofilms in ten North American streams. *Freshwater Biology* 48:1031–1049.

Thorp, J. H., and M. D. Delong. 2002. Dominance of autochthonous autotrophic carbon in food webs of heterotrophic rivers. *Oikos* 93:543–550.

Tromboni, F., S. A. Thomas, B. Gücker, V. Neres-Lima, C. Lourenço-Amorim, T. P. Moulton, E. F. Silva-Junior, R. Feijó-Lima, I. G. Boéchat, and E. Zandonà. 2018. Nutrient limitation and the stoichiometry of nutrient uptake in a tropical rain forest stream. *Journal of Geophysical Research: Biogeosciences* 123: 2154–2167.

Van Horn, D. J., R. L. Sinsabaugh, C. D. Takacs-Vesbach, K. R. Mitchell, and C. N. Dahm. 2011. Response of heterotrophic stream biofilm communities to a gradient of resources. *Aquatic Microbial Ecology* 64:149–161.

Vannote, R. L., G. W. Minshall, K. W. Cummins, J. R. Sedell, and C. E. Cushing. 1980. The River Continuum Concept. *Canadian Journal of Fisheries and Aquatic Sciences* 37:130–137.

Vonk, J. E., S. E. Tank, P. J. Mann, R. G. M. Spencer, C. C. Treat, R. G. Striegl, B. W. Abbott, and K. P. Wickland. 2015. Biodegradability of dissolved organic carbon in permafrost soils and aquatic systems: A meta-analysis. *Biogeosciences* 12:6915–6930.

Warren, D. R., S. M. Collins, E. M. Purvis, M. J. Kaylor, and H. A. Bechtold. 2017. Spatial variability in light yields colimitation of primary production by both light and nutrients in a forested stream ecosystem. *Ecosystems* 20:198–210.

Weishaar, J. L., G. R. Aiken, B. A. Bergamaschi, M. S. Fram, R. Fujii, and K. Mopper. 2003. Evaluation of specific ultraviolet absorbance as an indicator of the chemical composition and reactivity of dissolved organic carbon. *Environmental Science & Technology* 37:4702–4708.

Zall, D. M., D. Fisher, and M. Garner. 1956. Photometric determination of chlorides in water. *Analytical Chemistry* 28:1655–1668.

Ziegler, S. E., D. R. Lyon, and S. L. Townsend. 2009. Carbon release and cycling within epilithic biofilms in two contrasting headwater streams. *Aquatic Microbial Ecology* 55:285–300.

Zimov, S. A., S. P. Davydov, G. M. Zimova, A. I. Davydova, E. A. G. Schuur, K. Dutta, and F. S. Chapin. 2006. Permafrost carbon: Stock and decomposability of a globally significant carbon pool. *Geophysical Research Letters* 33:27484.